*Journal of The Electrochemical Society*, **160** (6) C189-C196 (2013)
0013-4651/2013/160(6)/C189/8/$31.00 © The Electrochemical Society


# Oxide Film Growth Kinetics on Metals and Alloys

## I. Physical Model

**Antoine Seyeux,[z] Vincent Maurice, and Philippe Marcus[*,z]**

*Laboratoire de Physico-Chimie des Surfaces, CNRS (UMR 7045), Ecole Nationale Supérieure de Chimie de Paris (Chimie ParisTech), 75005 Paris, France*

Oxide layers play a crucial role in the corrosion resistance of metals and alloys and the growth kinetics of these films is of major interest. To express the oxide growth kinetics, three main models are available: the Cabrera-Mott model, the Fehlner-Mott model and the Point Defect Model (PDM). These models are reviewed in the first part of the paper. Among these models, the PDM is the only one that takes into account the interfacial potential drops during the oxide growth. However, in this model: (i) no parameters relative to the substrate alloy are taken into account, and (ii) the growth is limited by the flow of oxygen vacancies through the film (transport *via* both cation interstitial and vacancy positions are not taken into account). Here we present a "generalized model" for the kinetics of oxide growth in which the evolution of the interfacial potential drops during oxide growth is included, as well as the variation of the electric field in the oxide during film growth. This new model allows us to describe the growth of oxide films on alloys under non-steady-state conditions. The link between oxide growth and cation release into the solution is also included.
 [DOI: 10.1149/2.036306jes] 

Manuscript submitted January 14, 2013; revised manuscript received February 27, 2013. Published March 13, 2013.

Passivity of metals is a central issue in corrosion science. Oxide films play a key role in the corrosion resistance of metals and alloys. The understanding of their growth kinetics requires a detailed knowledge of the involved interfacial reactions and transport mechanisms. Modeling oxide growth is a major issue for lifetime prediction in corrosion engineering. The phenomena identified to be involved in the formation of oxide films are: (i) the growth of the oxide layer, (ii) the dissolution of the oxide film and (iii) the precipitation of dissolving species from the solution, (ii) and (iii) being relevant for anodic oxide films only.

For the last sixty years, considerable efforts have been made in order to understand the elementary processes and the role of point defects (interstitials or vacancies) in the growth of oxide films. Three main models, all based on the Wagner theory,[1] have been proposed to express the growth kinetics of compact oxide film formed by solid-state diffusion on metals: (i) the Cabrera-Mott model,[2] (ii) the Fehlner-Mott model,[3] both initially developed to treat the case of oxide films formed thermally in air, and (iii) the Point Defect Model[4–6] (PDM), developed for electrochemically-formed oxide films. More recently, two additional models describing the growth of oxide films on alloys, have been published: the Mixed Conduction Model (MCM)[7,8] (extension of the PDM model allowing determining the electronic properties of the oxide layer) and an atomistic model[9] (including Kinetic Monte Carlo simulation of the oxide growth).

In classical models, experimental growth kinetics of oxide films formed in aqueous solution are fitted by the two following laws:[10–13]

$$x = A + B \ln t \text{(logarithmic law)} \quad [1]$$

$$\frac{1}{x} = C - D \ln t \text{(inverse logarithmic law)} \quad [2]$$

where x is the film thickness, t is the time, and A, B, C and D are constants. This dual behavior is not unexpected since the logarithmic and inverse logarithmic laws are known to be mathematically equivalent when the change in thickness is small, as illustrated by Lukac et al.[11]. The three classical growth models can describe such laws. The Fehlner-Mott and PDM models predict a logarithmic growth law, while the Cabrera-Mott model predicts an inverse logarithmic law for very thin oxide film growth ($\ll$ 10 nm) and a parabolic law for thicker oxide films. However, and as shown in the following, a detailed analysis of these models shows that some assumptions are questionable from a physical viewpoint, and an extended model with less restrictive assumptions is needed to describe the growth of oxide films on metals and alloys in aqueous solution.

In this paper we present a short critical review of the existing growth models and, as an alternative, we propose an extended macroscopic model accounting more accurately for the role of interfacial potential drops and that can be used to describe the growth of oxide films on alloys. Finally the model will be compared to experimental kinetics data compiled for Alloy 690 in high temperature and high pressure water.

### Critical Review of the Existing Models

It is known that the driving force for oxide formation in a metal/oxide/electrolyte system (i.e. the potential drop V) is divided into three parts (Figure 1): (i) the potential drop at the metal/oxide interface ($\phi_{m/f}$) that controls the internal interfacial reactions, (ii) the potential drop at the oxide/electrolyte interface ($\phi_{f/s}$) that controls the external interfacial reactions and (iii) the potential drop in the oxide layer ($\phi_f$) that controls the transport mechanisms across the oxide film. Thus, the oxide layer is the result of complex processes combining transport through the oxide and interfacial reactions.

Figure 2 shows a list of all the processes that should be considered in the metal/oxide/electrolyte system during the growth of an oxide film. Each growth model (Cabrera-Mott, Fehlner-Mott and PDM)

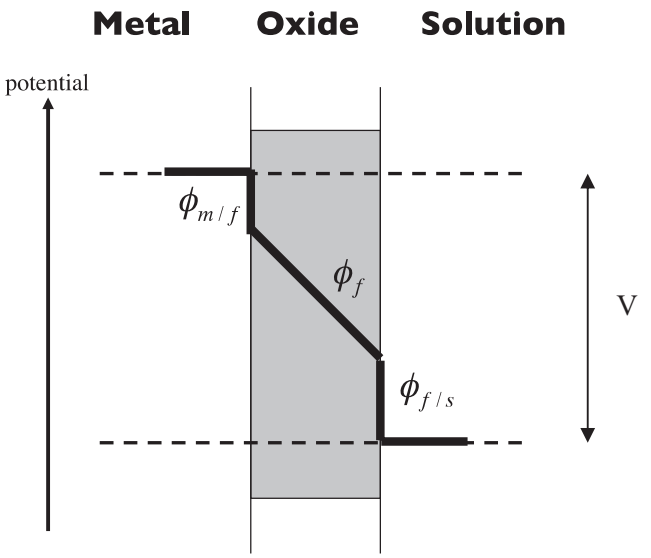


**Figure 1.** Scheme of the potential drop in the metal/oxide/solution system.

*Electrochemical Society Fellow.
[z]E-mail: antoine-seyeux@chimie-paristech.fr; philippe-marcus@chimie-paristech.fr

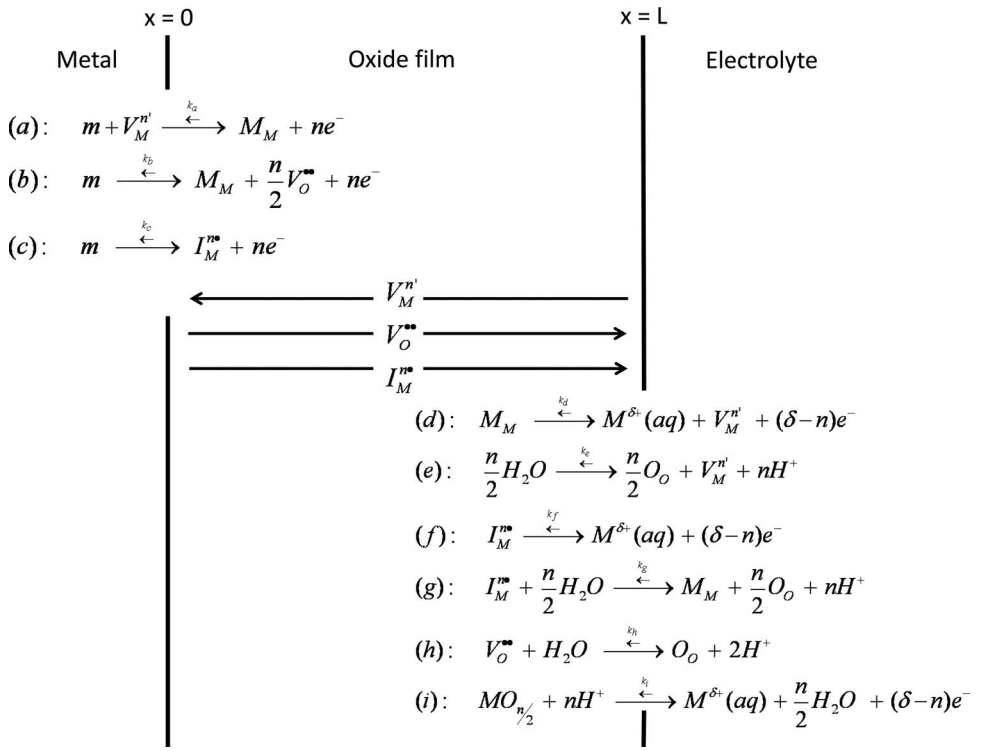


**Figure 2.** Scheme describing the reaction and transport processes involved in the system metal/oxide/electrolyte during the growth of the oxide layer. Oxygen vacancies, metallic vacancies and metallic interstitials are implied. The dissolution of the oxide film is also taken into account. The Kröger-Vink notation is used to describe the defects. (a) cation injection into cation vacancy position of the oxide at the metal/oxide interface, (b) oxygen vacancies formation in the oxide at the metal/oxide interface, (c) cation injection in interstitial position of the oxide at the metal/oxide interface, (d) cation dissolution via cation vacancies at the oxide/electrolyte interface, (e) formation of cation vacancies in the oxide at the oxide/electrolyte interface, (f) cation dissolution via interstitial position at the oxide/electrolyte interface, (g) growth of the oxide *via* interstitial positions at the oxide/electrolyte interface, (h) injection of oxygen in anionic vacancy position at the oxide/electrolyte interface, and (i) dissolution of the oxide at the oxide/electrolyte interface.

includes some of these reactions as detailed in the following. Only the PDM includes the interfacial potential drops, but the oxide/solution potential drop and the electric field in the oxide are assumed to remain constant during oxide growth.

A compilation of the main characteristics of the three models for oxide growth on metals is given in Table I:.

*Cabrera-Mott model*[2].— The main assumptions of this model are the following:

(i) The oxide growth is due to the transport, via interstitial positions, of cations across the oxide film (transport ($I_M$) in Figure 2) to the oxide/solution interface where they react with the electrolyte (reaction (g) in Figure 2).
(ii) The activation energy of the rate-limiting step is reduced by the electric field F set up in the oxide film ($F = \phi_{f/x}$).
(iii) For weak electric field (thick oxide films), the limiting step is assumed to be the transport of cations through the oxide (transport $I_M$ in Figure 2), which leads to a parabolic growth law ($x = \sqrt{Et}$, where E is a constant).

**Table I. Comparative summary of the main characteristics of the Cabrera-Mott, Fehlner-Mott and PDM models.**

| | Mott-Cabrera model (air formation) | Fehlner-Mott model (air formation) | Point Defect Model Macdonald (electrochemical formation) |
|---|---|---|---|
| Growth mechanism | Migration of interstitial cations | Migration of interstitial anions | Migration of anion vacancies |
| Growth law | Weak electric field<br>$x^2 = Et$<br>Strong electric field<br>$1/x = C - D\ln t$ | Activation energy function of thickness<br>$x = A + B\ln(t + t_0)$ | Transport controlled<br>$x = \frac{1}{2K}[\ln 2KA(B-1) + \ln t]$<br>Interface controlled<br>$x = x_{t=0} + \frac{1}{b}\ln\left[1 + Ab\exp[-bx_{t=0}]t\right]$ |
| Limiting step | Weak electric field<br>Transport of cations through the film<br>Strong electric field<br>Injection of cations at the metal/oxide interface | Anion transport<br>Through the film | Transport control<br>Oxygen vacancies<br>Interface control<br>Anion vacancies injection at the metal/oxide interface |
| Electric field | Function of layer thickness<br>(E = V/L) | Independent of thickness | Independent of thickness |
| Dissolution | | | Dissolution of oxide<br>Dissolution of metal |
| Crystalline defects in oxide layer (grain boundaries) | No | Modification of the growth law (grain boundaries) | No |
| Interfacial potential | No | No | Function of pH and $V_{ext}$ |

(iv) For strong electric field (thin oxide films), the limiting step is assumed to be the injection of cations at the metal/oxide interface (reaction (c) in Figure 2), which leads to an inverse logarithmic growth law (Eq. 2).

By using non-stationary state equations this model appears to be appropriate for describing the oxide film growth. However, there are limitations to its application to metal/oxide/solution interfacial systems. Indeed, in this model, the following points are not taken into consideration:

1. The potential drop at the oxide/electrolyte interface. This potential drop, responsible for the dissolution of the oxide film according to reaction (i) in Figure 2, is not considered, the model having initially been developed to describe oxides formed in air. Consequently, the pH of the solution is not taken into account to express the oxide growth kinetics, although it is known to affect it.
2. The potential drop at the metal/oxide interface. In the case of growth controlled by the injection of cations at the metal/oxide interface, the authors assume that the potential drop in the film ($\phi_f$) reduces the activation energy of the rate-limiting step, and not the potential drop at the metal/oxide film interface ($\phi_{m/f}$).
3. The presence of vacancies in the oxide. The model assumes that the transport of cations proceeds exclusively *via* interstitial positions. However, vacancies can also be involved in the growth mechanism.
4. The possible anionic growth of the oxide.
5. The composition of the metallic substrate. This model only describes oxide film growth on pure metals (the composition of the alloy under the oxide film is not taken into account in the model).

*Fehlner-Mott model*[3].— The Fehlner-Mott model was intended as an evolution of the Cabrera-Mott model and is based on similar assumptions. The differences are the following:

(i) The transport of interstitial anions across the oxide film to the metal/oxide interface is assumed to be responsible for the oxide growth (not shown in Figure 2).
(ii) The transport of the anions in the film is assumed to be the only rate-limiting step and it is assisted by the electric field.
(iii) The electric field is assumed to be independent of the oxide thickness ($F$ = constant).
(iv) The activation energy of the rate-limiting step (transport of anions across the film) is assumed to increase linearly with the oxide thickness ($W_A = W^\circ + \mu x$, where $W^\circ$ and $\mu$ are constants for a given oxide structure). This assumption comes from the idea, originally proposed by Eley and Wilkinson[14] in 1960, that logarithmic growth laws can be obtained by assuming any mechanism whose activation energy increases linearly with the oxide thickness. This assumption is not correct since the activation energy should depend on the structure but not on the oxide thickness.

Based on these new assumptions, the Fehlner-Mott model predicts a logarithmic growth law ($x = A + B\ln(t + t_0)$ where A and B are parameters depending on $\mu$ and $t_0$).

The limits of the Fehlner-Mott model are similar to those listed previously for the Cabrera-Mott model. This model does not take into consideration:

1. The potential drop at the oxide/electrolyte interface (i.e. the dissolution of the oxide).
2. The potential drop at the metal/oxide interface.
3. The presence of vacancies in the oxide.
4. The cationic growth of the oxide.
5. The composition of the metallic substrate.

This model does not allow a good description of anodically-formed oxide films. Indeed, as it is assumed that the electric field is independent of the oxide thickness ($F$ = constant) and since the interfacial potentials are not considered, the electric field should be defined as $F = \frac{V_{app}}{x}$ where $V_{app}$ is the applied potential to describe the case of anodically-formed oxide films. However $V_{app}$ is constant and thus the electric field cannot remain constant during the oxide growth. Finally, this model is built on assumptions (e.g. oxide grows by the migration of anions *via* interstitial positions, the activation energy of the rate-limiting step (transport of anions across the film) increases linearly with the oxide thickness) that do not reflect a correct physical description of the mechanisms involved. The migration of anions *via* interstitial positions seems somewhat unrealistic because of steric hindrance in the oxide network (although it may be valid at intergranular boundaries of the oxide film).

*Point defects model (PDM)*[4–6].— This model was developed by Macdonald et al. in 1981 to describe the growth of electrochemically-formed oxide films. In its original version,[4] the main assumptions of this model are:

(i) The transport of anionic vacancies across the oxide film to the oxide/solution interface is responsible for oxide growth (transport $V_O$ in Figure 2).
(ii) The diffusion of interstitial cations and/or cation vacancies results only in metal dissolution, following reactions (f) and (d) on Figure 2, respectively.
(iii) The transport of the anionic vacancies is the rate-limiting step of the oxide growth.
(iv) The electric field is assumed to be independent of the oxide thickness ($F$ = constant).

The main asset of this model is that the interfacial potential drops ($\phi_{m/f}$ and $\phi_{f/s}$) are taken into consideration. They are assumed to be functions of the pH and the applied potential $V_{app}$. Point defect transport is described by the Fick equation and a logarithmic law (Eq. 1) is obtained for the growth rate where A is a function of the pH, the applied potential $V_{app}$ and the electric field in the oxide film.

Macdonald et al. later extended this model to the case of growth controlled by the interfacial reactions.[5] This model gave another logarithmic growth law, which is function of the pH and the applied potential ($V_{app}$).

The dissolution of the oxide film at the oxide/electrolyte interface, following reaction (i) in Figure 2, is also considered in this model. The rate of the oxide film dissolution is given by: $v = k_s[H^+]^m$ where $k_s$ is the rate constant, depending on the potential drop at the oxide/electrolyte interface (i.e. function of the applied potential $V_{app}$) and $m$ the order of the reaction. The oxide film reaches a stationary thickness when the oxide growth rate and the dissolution rate are equal.

This model was the first one to consider the interfacial potential drops to describe anodic oxide film growth on metals. Simplifying assumptions made in the model are as follows:

1. In its original version, the model assumes that a constant potential drop ($\phi_{f/s}$) is maintained at the oxide/electrolyte interface during the oxide growth. This assumption implies that, at the oxide/electrolyte interface, the reaction $O_{oxide} + 2H^+ \xleftrightarrow{} H_2O$ is faster than the rate-limiting step (transport of species through the film) and that an equilibrium is maintained at this interface during the oxide growth. This assumption would be valid for stationary conditions (i.e. when the oxide growth rate is equal to the dissolution rate) when the interfacial potential drops $\phi_{m/f}$ and $\phi_{f/s}$ are imposed by the structure of the metal/oxide interface and the Nernst equilibrium, respectively. However these interfacial potential drops should evolve during the oxide growth (i.e. under non stationary conditions).
2. At the equilibrium state for the oxide/electrolyte interface, the interfacial potential drop $\phi_{f/s}$ is assumed to be function of the applied potential. At the equilibrium state, the oxide/electrolyte potential drop is given by the Nernst equilibrium only (it is not a function of the applied potential).

3. The metal/oxide potential drop appears to be a function of the pH of the electrolyte. The metal/oxide potential drop should not be a function of the pH of the electrolyte. It should be imposed by the structure of the metal/oxide interface only.
4. A constant electric field in the film is assumed, although it should vary during film growth (non stationary conditions).
5. The oxide growth by cation migration via interstitial or vacancy positions is not included.
6. The composition of the metallic substrate is not taken into account (which would be necessary for the case of alloys).

Bojinov et al. adapted the formalism of the PDM to the case of alloys by developing the mixed conduction model (MCM), which emphasizes the coupling between ionic and electronic defects in quasi-steady-state passive films.[7,8] It allowed the authors to determine the electronic properties of the oxide layer, the main kinetic and transport parameters to calculate the steady-state current density, the oxide film impedance response and the thickness vs. time relationship on many alloys. However, as in the PDM model, quasi-steady-state approximation is used although the oxide growth takes place under non-stationary conditions. Moreover, as discussed previously, the interfacial potential drop at the oxide/film interface and the electric field in the oxide are assumed to remain constant during the oxide growth, which is associated to stationary conditions, although non-stationary condition must prevail for oxide growth.

From a kinetics viewpoint, the equations describing the growth of the oxide film are the same to the ones established by Macdonald in the PDM. Our paper being focused on the oxide growth kinetics, no further detailed description of this model will be done in this review, as the major contribution of the MCM model is the description of the electronic properties of the oxide film.

Three models for oxide film growth, i.e. the Cabrera-Mott, Fehlner-Mott and PDM models have been reviewed above. Each model is based on specific assumptions that have been discussed.

The above critical review points out important limitations of these models. Among them, the use of quasi-steady-state approximation to describe the oxide growth that takes place under non-stationary conditions, the absence of parameters relative to the substrate for alloys (except for the MCM), and the fact that the growth of the film by transport *via* cation interstitials or cation vacancy positions is not included appear as common serious limitations. As for the PDM model, it takes into account the interfacial potentials, but the potential drop at the oxide/film interface and the electric field in the oxide are assumed to remain constant during the oxide growth.

## Generalized Model for Oxide Film Growth

A "generalized model" taking into account the interfacial potential drops and their evolution during the oxide growth (i.e under non stationary conditions) is proposed below to express the kinetics of oxide growth on alloys. In this model, all the reactions involved in the oxide growth, and listed in Figure 2, are considered. The formalism is then applied to the case of stainless alloys. The numerical simulation is the purpose of a second paper.[15]

*Relationship between the global potential, the potential drop in the oxide layer and the interfacial potential drops.*— As shown in Figure 1, the potential drop (V) in a metal/oxide/electrolyte system is divided into three potential drops, $\phi_{m/f}$, $\phi_{f/s}$ and $\phi_f$, following the relation $V = \phi_{m/f} + \phi_f + \phi_{f/s}$. During the oxide film growth, the potential drops $\phi_{m/f}$, $\phi_{f/s}$ and $\phi_f$ vary until they reach a stationary value when the oxide film reaches a stationary thickness. Thus, in non-stationary conditions (film growth), the potential drops $\phi_{m/f}$, $\phi_{f/s}$ and $\phi_f$ are functions of the oxide thickness (x) and can be expressed as $\phi_{m/f}(x)$, $\phi_{f/s}(x)$ and $\phi_f(x)$. When an oxide film, with a stationary thickness $x_i$, is subjected to a potential variation $\Delta V$ (that can be due to e.g. a modification of the electrolyte chemistry or temperature), the potential drops $\phi_{m/f}(x)$, $\phi_{f/s}(x)$ and $\phi_f(x)$ are modified and the oxide film thickness (with initial thickness $x_i$) evolves up to a new stationary

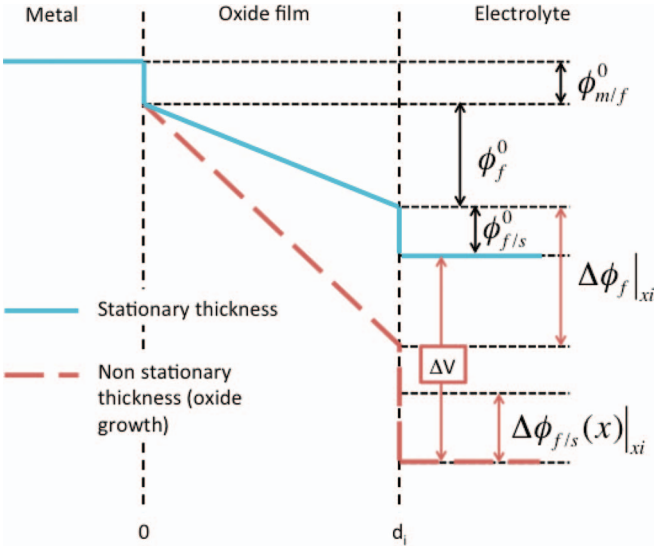


**Figure 3.** Model for the evolution of the potential drops for a metal/oxide/electrolyte system after a potential modification (ΔV).

thickness $x_f$ (see Figure 3). Assuming that the potential drop at the metal/oxide interface ($\phi_{m/f}$) is constant during the oxide growth (i.e. the structure of the inner layer and the composition of the alloy below the oxide are assumed to remain unchanged during the growth) and that $\phi_{f/s}(x)$ decreases during the growth of the oxide, the potential drops can be expressed as:

$$\begin{aligned}
&\phi_{m/f}(x) = \phi^0_{m/f}(x_i) = \text{constant} \\
&\phi_{f/s}(x) = \phi^0_{f/s}(x_i) + \Delta\phi_{f/s}(x) = \phi^0_{f/s}(x_i) + \alpha f(x)\Delta V \\
&\phi_f(x) = \phi_f(x_i) + \Delta\phi_f(x) = \phi_f(x_i) + (1 - \alpha f(x))\Delta V
\end{aligned} \quad [3]$$

where α ($0 \le \alpha \le 1$) is a constant for a given system reflecting the fraction of the potential ΔV applied to the metal/oxide interface, $\phi^0_{f/s}$ is a constant corresponding to the Nernst equilibrium at the oxide/electrolyte interface ($O^{2-} + 2H^+ \overleftarrow{\longrightarrow} H_2O$), $x_i \le x \le x_f$ and $f(x_f) = 0 \le f(x) \le 1 = f(x_i)$, where f(x) is a decreasing function reflecting the variation of the potential drop at the metal/oxide interface during the oxide growth.

*Oxide film growth law.*— In order to express the growth kinetics for oxide layers on metals and alloys, two cases must be considered: (i) the growth is controlled by the transport of charged species through the oxide, or (ii) the growth is controlled by the injection of cations at the metal/oxide interface.

*Growth controlled by the transport of charged species through the oxide.*—In this part, it is considered that the cathodic reaction (electron consumption) is not the limiting step for oxide growth. Thus, if the growth is controlled by the transport of charged species through the oxide, the oxide growth kinetics is given by the flow of charged species (interstitials or vacancies) across the oxide. In the presence of both concentration and potential gradients, the flow can be determined from the generalized Fick's first law:

$$J_i = D_i^* \frac{\partial C_i}{\partial d} + D_i^* \frac{C_i}{RT} q_i \mathcal{F} \frac{\partial \phi}{\partial d} \quad [4]$$

where $J_i$ is the flux of species i per unit area per unit time, $D_i^*$ and $C_i$ are the diffusion coefficient and the concentration of charged species i in the oxide, respectively, and d is a position in the oxide of thickness x.

For any oxide film thickness, a linear potential drop is considered in the oxide film (meaning that there is no excess charge within the oxide) as in the work of Macdonald et al.[4] Combining Eq. 3 and 4, the

flow of species diffusing through the oxide film can be expressed as:

$$J_i = q_i \frac{\mathcal{F}\left[\phi_f^0 + \Delta V\,(1-\alpha f(x))\right]}{RTx} D_i^* \frac{C_i|_{m/f} \exp\left[q_i \frac{\mathcal{F}\phi_f(x)}{RT}\right] - C_i|_{f/s}}{\exp\left[q_i \frac{\mathcal{F}\phi_f(x)}{RT}\right] - 1}$$

$$= q_i \frac{\mathcal{F}\phi_f(x)}{RTx} D_i^* \frac{C_i|_{m/f} \exp\left[q_i \frac{\mathcal{F}\left[\phi_f^0 + \Delta V(1-\alpha f(x))\right]}{RT}\right] - C_i|_{f/s}}{\exp\left[q_i \frac{\mathcal{F}\left[\phi_f^0 + \Delta V(1-\alpha f(x))\right]}{RT}\right] - 1} \quad [5]$$

where $C_i|_{m/f}$ and $C_i|_{f/s}$ are the concentrations of species i (in units of number of species/m$^3$) at the metal/oxide and oxide/electrolyte interfaces, respectively.

Our hypothesis for the generalized model is that the potential across the film is a linear function of position, d. This assumption holds for both transient and steady states, but the gradient of the linear function will evolve during the transient. From this assumption it follows that the electric field strength F is constant throughout the film because F = ∂ϕ f / ∂d, although F decreases during film growth. Fick's law is also simplified by the assumption that the concentration throughout the film is a linear function of the position, d. The hypothesis on the concentration profile is likely to be justified in the middle of the film, but border effects are neglected.

*Growth controlled by the injection of cations at the metal/oxide interface.*—The situation is different in the case where the growth is controlled by the injection of cations at the metal/oxide interface. The growth rate is then governed by the flow of species going through the interface. The case of cation species going through the interface into interstitial positions of the oxide will be treated in the following (reaction (c) in Figure 2). A similar treatment can be used in the case of cation species going across the interface into cation vacancy positions in the oxide (reaction (a) in Figure 2), and in the case of injection of oxygen vacancies (reaction (b) in Figure 2).

If cations diffuse through the metal/oxide interface, vacancies are produced in the metal following the relation (reaction (c) in Figure 2):

$$m \longrightarrow I_M^{n\bullet} + ne^- \quad [6]$$

Following Cabrera and Mott,[2] the probability for a cation to escape the metal and reach an interstitial position can be expressed as:

$$\nu \exp\left[-\frac{W_I^M - en\phi_{m/f}}{kT}\right] \quad [7]$$

where ν is the vibration frequency of M and $W_I^M$ is the activation energy of reaction 13.

In this expression, it is assumed that the potential drop at the metal/oxide interface, and not the potential drop in the film, reduces the activation energy of the process and thus facilitates the diffusion of cations through the interface.[16]

Accordingly, the flow of cations at the metal/oxide interface is given by:

$$J_{I_M}^M\big|_{m/f} = \nu C_m^M \exp\left[-\frac{W_I^M - en\phi_{m/f}}{kT}\right] \quad [8]$$

where $C_m^M$ is the concentration of M in the metal.

Since $\phi_{m/f}^0$ is independent of the oxide thickness (see above), the flow of species diffusing through the metal/oxide interface is constant. Thus, the kinetics of the oxide film growth can be expressed as:

$$\frac{dx}{dt} = \frac{\Omega}{N_V} J_{I_M}^M\big|_{m/f} = \nu C_m^M \exp\left[-\frac{W_I^M - en\phi_{m/f}}{kT}\right] \quad [9]$$

where $N_V$ is Avogadro's number and Ω is the molar volume of oxide per Cr cation. This leads to the following linear growth law:

$$x = A' C_m^M t \quad [10]$$

with $A' = \frac{\Omega}{N_V} \nu \exp\left[-\frac{W_I^M - en\phi_{m/f}}{kT}\right]$.

It is important to note here that the case of growth controlled by the injection of cations at the metal/oxide interface occurs only if a very strong electric field exists in the oxide. This may happen for ultra thin oxide films with thicknesses up to a few nanometres.[†]

*Dissolution of the oxide film.*—Considering that film dissolution takes place at the film/solution interface, it follows reaction (i) on Figure 2:

$$MO_{n/2} + nH^+ \underset{k_i}{\longrightarrow} M^+(aq) + \frac{n}{2}H_2O + (\delta - n)e^- \quad [11]$$

which is a lattice non-conservative reaction (the thickness of the film is decreased). This equation allows to treat either electrochemical or chemical dissolution depending on δ.

Thus, as previously shown by Macdonald et al.,[4] the dissolution rate can be expressed as:

$$v_{diss} = k_s \left[H^+\right]^m \quad [12]$$

where $k_s$ is the solubility constant of the oxide and $m$ is the reaction order with respect to the $H^+$ ions.

According to the Arrhenius law, $k_s$ can be expressed as:

$$k_s = k^\circ \exp\left[-\frac{E_A}{kT}\right] \quad [13]$$

where $E_A$ is the activation energy of equation 12 and $k^\circ$ is a pre-exponential factor.

At the oxide/solution interface, the potential drop $\phi_{f/s}(x)$ leads to the reduction of the activation energy ($E_A$) for the dissolution reaction. Thus, the dissolution of the oxide is facilitated and the dissolution rate can be expressed as:

$$v_{diss} = k_s \left[H^+\right]^m = k^\circ \exp\left[-\left(\frac{E_A}{kT} - \frac{e\phi_{f/s}(x)}{kT}\right)\right]\left[H^+\right]^m \quad [14]$$

$$v_{diss} = k^\circ \exp\left[-\left(\frac{E_A}{kT} - \frac{e\left(\phi_{f/s}^\circ(d_i) + \alpha f(x)\Delta V\right)}{kT}\right)\right]\left[H^+\right]^m \quad [15]$$

Consequently, the dissolution rate of the oxide will evolve during the growth of the oxide film. Moreover, it is function of the pH, of the structure of the oxide film ($\phi_{f/s}(x)$ is function of the structure[16]) and of the applied potential (see Eq. 3). In stationary conditions, the oxide film growth rate will be equal to the dissolution rate.

*Application to the case of oxide film growth on stainless alloys in high temperature water.*— The model presented above is now applied to the case of oxide films formed on stainless alloys in high temperature water by transport of charged species through the oxide. The following hypotheses are made:

(i) Oxide growth is controlled by the migration of species through the oxide. The reactions involving interstitials or vacancies are under equilibrium at both interfaces.
(ii) A pure chromium oxide film ($Cr_2O_3$) is formed on stainless alloys. This assumption is based on experimental data showing the formation of an internal $Cr_2O_3$ barrier layer on stainless alloys oxidized in high temperature water.[17–23]
(iii) There is no interaction between the flow of Cr, Fe and Ni ions (i.e. the vacancy concentration in the film is high).
(iv) All Cr ions are consumed by the growth of the oxide (i.e. there is no chromium dissolution).
(v) All Fe and Ni ions are dissolved in the solution (i.e. they do not participate in oxide growth).

The different reactions involving Cr, Fe and Ni at both interfaces are listed in Figure 4. The concentration of species at both interfaces can be expressed using the standard Gibbs energy and the electrochemical

[†]As an example, in the case of oxide film growth in high temperature water, such thicknesses correspond, according to the work of Machet et al.[17] on Alloy 800, to approximately 5 minutes of oxidation time. For longer oxidation times, the growth is controlled by the transport of species through the previously developed oxide film.

| | Metal/Oxide interface | Oxide/Electrolyte interface |
|---|---|---|
| Cr | 1) $Cr\|_{alloy} \xrightarrow{\leftarrow} M_{Cr} + \frac{3}{2}V_O^{\bullet\bullet} + 3e^-$<br>2) $Cr\|_{alloy} + V_{Cr}^{'''} \xrightarrow{\leftarrow} M_{Cr} + 3e^-$<br>3) $Cr\|_{alloy} \xrightarrow{\leftarrow} I_{Cr}^{\bullet\bullet\bullet} + 3e^-$ | 8) $V_O^{\bullet\bullet} + H_2O \xrightarrow{\leftarrow} O_O + 2H^+$<br>9) $M_{Cr} + \frac{3}{2}H_2O \xrightarrow{\leftarrow} \frac{3}{2}O_O + M_{Cr} + V_{Cr}^{'''} + 3H^+$<br>10) $I_{Cr}^{\bullet\bullet\bullet} + \frac{3}{2}H_2O \xrightarrow{\leftarrow} \frac{3}{2}O_O + M_{Cr} + 3H^+$ |
| Fe | 4) $Fe\|_{alloy} + V_{Cr}^{'''} \xrightarrow{\leftarrow} M_{Fe} + 3e^-$<br>5) $Fe\|_{alloy} \xrightarrow{\leftarrow} I_{Fe}^{\bullet\bullet\bullet} + 3e^-$ | 11) $M_{Fe} \xrightarrow{\leftarrow} V_{Cr}^{'''} + Fe^{3+}$<br>12) $I_{Fe}^{\bullet\bullet\bullet} \xrightarrow{\leftarrow} Fe^{3+}$ |
| Ni | 6) $Ni\|_{alloy} + \frac{2}{3}V_{Cr}^{'''} \xrightarrow{\leftarrow} M_{Ni} + 2e^-$<br>7) $Ni\|_{alloy} \xrightarrow{\leftarrow} I_{Ni}^{\bullet\bullet} + 2e^-$ | 13) $M_{Ni} \xrightarrow{\leftarrow} \frac{2}{3}V_{Cr}^{'''} + Ni^{2+}$<br>14) $I_{Ni}^{\bullet\bullet} \xrightarrow{\leftarrow} Ni^{2+}$ |

**Figure 4.** Application of the generalized model to stainless alloys (containing Fe, Cr, Ni): reactions at the metal/oxide and oxide/electrolyte interfaces.

potential as already shown by Macdonald et al. for a metal.[4] They are listed in Figure 5. The flow of oxygen vacancies, as well as the flow of Cr, Fe and Ni *via* interstitial and vacancy positions can be expressed. According to our assumptions the oxide film growth flow can be expressed as follows:

$$J_{growth} = J_{M_{Cr}} + J_{I_{Cr}} + J_{V_O} \quad [16]$$

and the metal release flow can be expressed as:

$$J_{release} = J_{M_{Fe}} + J_{I_{Fe}} + J_{M_{Ni}} + J_{I_{Ni}} \quad [17]$$

The oxide growth kinetics, taking into account the variations of the potential drops in the metal/oxide/electrolyte system during the oxide film growth, can be determined by numerical integration of the following expression:

$$\frac{dx}{dt} = \frac{\Omega}{N_V} j_{growth} = \frac{\Omega}{N_V}\left(J_{M_{Cr}} + J_{I_{Cr}} + J_{V_O}\right) \quad [18]$$

As an example, the flow of oxygen vacancies in the oxide film is treated below. The flow of cations *via* interstitial or vacancy positions could easily be expressed in a similar way.

$$= \frac{N_V}{\Omega}\exp\left[\frac{\Delta G_8^\circ - 2\mathsf{F}\left[\phi_{f/s}^0 + \Delta V \alpha f(x)\right]}{RT} - 4,606pH\right] \quad [19]$$

Where $\Delta G_1^0$ and $\Delta G_8^0$ correspond to the standard Gibbs energy of reactions 1 and 8 in Figure 4, respectively:

$$Cr|_{alloy} \xrightarrow{\leftarrow} M_{Cr} + \frac{3}{2}V_{\ddot{O}}^{\bullet\bullet} + 3e^- \quad [20]$$

$$V_{\ddot{O}}^{\bullet\bullet} + H_2O \xrightarrow{\leftarrow} 2H^+ + O_O \quad [21]$$

It is important to note that in these expressions, in contrast with the PDM, the potential drops ($\phi_{f/s}$(x) and $\phi_f$(x)) and electric field are functions of the oxide film thickness and thus vary during film growth. Consequently $C_{V_{\ddot{O}}}|_{m/f}$ and $C_{V_{\ddot{O}}}|_{f/s}$ are also functions of the oxide thickness.

The flow of oxygen vacancies in the oxide film is expressed as:

$$J_{V_O} = \frac{N_V}{\Omega} q_{V_O} \frac{\mathsf{F}\left[\phi_f^0 + \Delta V\,(1-\alpha f(x))\right]}{RTx} D_{V_O}^* \cdot \frac{\exp\left[\frac{-\frac{2}{3}\Delta G_1^\circ + 2\mathsf{F}\left[\phi_{m/f}^0\right]}{RT} + \frac{3}{2}\ln x_{Cr}\right]\exp\left[q_{V_O}\frac{\mathsf{F}\left[\phi_f^0 + \Delta V(1-\alpha f(x))\right]}{RT}\right] - \exp\left[\frac{\Delta G_8^\circ - 2\mathsf{F}\left[\phi_{f/s}^0 + \Delta V\alpha f(x)\right]}{RT} - 4,606pH\right]}{\exp\left[q_{V_O}\frac{\mathsf{F}\left[\phi_f^0 + \Delta V(1-\alpha f(x))\right]}{RT}\right] - 1} \quad [22]$$

As discussed above, the concentration of oxygen vacancies ($C_{V_{\ddot{O}}}$) at both interfaces can be expressed as:

$$C_{V_O}|_{m/f} = \frac{N_V}{\Omega}\exp\left[\frac{-\frac{2}{3}\Delta G_1^\circ + 2\mathsf{F}\phi_{m/f}}{RT} + \frac{2}{3}\ln x_{Cr}\right]$$

$$C_{V_O}|_{f/s} = \frac{N_V}{\Omega}\exp\left[\frac{\Delta G_8^\circ - 2\mathsf{F}\phi_{f/s}(x)}{RT} - 4,606pH\right]$$

The "generalized model" developed above, by taking into account the interfacial potentials and their evolution during the oxide growth and including all the reactions involved in the oxide growth (transport of anion and cation *via* interstitial and vacancy positions is to our knowledge the first model capable of describing the growth of oxide films on alloys in aqueous solution under non steady-state conditions. Moreover, this model, by taking into account both the oxide growth and the release of species into the solution, is the first one including the link between these two phenomena.

## *Metal/Oxide interface*

(a)

$$C_{V_O} = \exp\left[\frac{-\frac{2}{3}\Delta G_1^0 + 2\mathcal{F}\phi_{m/f}}{RT} + \frac{3}{2}\ln x_{Cr}\right]$$

$$C_{V_{Cr}} = \exp\left[\frac{\Delta G_2^0 - 3\mathcal{F}\phi_{m/f}}{RT} - \ln x_{Cr}\right]$$

$$C_{M_{Fe}} = \left\{\exp\left[\frac{-\Delta G_4^0 + 3\mathcal{F}\phi_{m/f}}{RT}\right]\right\}. x_{Fe}.C_{V_{Cr}}$$

$$C_{M_{Ni}} = \left\{\exp\left[\frac{-\Delta G_7^0 + 2\mathcal{F}\phi_{m/f}}{RT}\right]\right\}. x_{Ni}.\left(C_{V_{Cr}}\right)^{\frac{2}{3}}$$

$$C_{M_{Cr}} = C_{tot}\big|_M - \left(C_{M_{Fe}} + C_{M_{Ni}} + C_{V_{Cr}}\right)$$

$$C_{I_{Cr}} = \left\{\exp\left[\frac{-\Delta G_3^0 + 3\mathcal{F}\phi_{m/f}}{RT}\right]\right\}. x_{Cr}.C_{V_I}$$

$$C_{I_{Fe}} = \left\{\exp\left[\frac{-\Delta G_5^0 + 3\mathcal{F}\phi_{m/f}}{RT}\right]\right\}. x_{Fe}.C_{V_I}$$

$$C_{I_{Ni}} = \left\{\exp\left[\frac{-\Delta G_6^0 + 2\mathcal{F}\phi_{m/f}}{RT}\right]\right\}. x_{Ni}.C_{V_I}$$

$$C_{V_I} = \frac{C_{tot}\big|_I}{1 + x_{Cr}\exp\left[\frac{-\Delta G_3^0 + 3\mathcal{F}\phi_{m/f}}{RT}\right] + x_{Fe}\exp\left[\frac{-\Delta G_5^0 + 3\mathcal{F}\phi_{m/f}}{RT}\right] + x_{Ni}\exp\left[\frac{-\Delta G_6^0 + 2\mathcal{F}\phi_{m/f}}{RT}\right]}$$

## *Oxide/Electrolyte interface*

(b)

$$C_{V_O} = \exp\left[\frac{\Delta G_8^0 - 2\mathcal{F}\phi_{f/s}(x)}{RT} - 4.606\,pH\right]$$

$$C_{V_{Cr}} = \exp\left[\frac{-\Delta G_9^0 + 3\mathcal{F}\phi_{f/s}(x)}{RT} + 6.909\,pH\right]$$

$$C_{M_{Fe}} = \left\{\exp\left[\frac{\Delta G_{11}^0 - 3\mathcal{F}\phi_{f/s}(x)}{RT}\right]\right\}. C_{V_{Cr}}.C_{Fe^{3+}(aq)}$$

$$C_{M_{Ni}} = \left\{\exp\left[\frac{\Delta G_{14}^0 - 2\mathcal{F}\phi_{f/s}(x)}{RT}\right]\right\}. C_{V_{Cr}}.C_{Ni^{2+}(aq)}$$

$$C_{M_{Cr}} = C_{tot}\big|_M - \left(C_{M_{Fe}} + C_{M_{Ni}} + C_{V_{Cr}}\right)$$

$$C_{I_{Cr}} = \left\{\exp\left[\frac{\Delta G_{10}^0 - 3\mathcal{F}\phi_{f/s}(x)}{RT} - 6.909\,pH\right]\right\}. C_{V_I}$$

$$C_{I_{Fe}} = \left\{\exp\left[\frac{\Delta G_{12}^0 - 3\mathcal{F}\phi_{f/s}(x)}{RT}\right]\right\}. C_{V_I}.C_{Fe^{3+}(aq)}$$

$$C_{I_{Ni}} = \left\{\exp\left[\frac{\Delta G_{13}^0 - 2\mathcal{F}\phi_{f/s}(x)}{RT}\right]\right\}. C_{V_I}.C_{Ni^{2+}(aq)}$$

$$C_{V_I} = \frac{C_{tot}\big|_I}{1 + \exp\left[\frac{\Delta G_{10}^0 - 3\mathcal{F}\phi_{f/s}(x)}{RT} - 6.909\,pH\right] + C_{Fe^{3+}(aq)}\exp\left[\frac{\Delta G_{12}^0 - 3\mathcal{F}\phi_{f/s}(x)}{RT}\right] + C_{Ni^{2+}(aq)}\exp\left[\frac{\Delta G_{13}^0 - 2\mathcal{F}\phi_{f/s}(x)}{RT}\right]}$$

**Figure 5.** Application of the generalized model to stainless alloys: concentrations of the different species at the metal/oxide interface (a), and the oxide/electrolyte interface (b). $\Delta G_i^0$ is the standard Gibbs energy of reaction i (defined on Figure 4).

## Conclusions

A critical review of the three main models for oxide film growth on metals (Cabrera-Mott, Fehlner-Mott and PDM) has been made. It appears that there is a need for a more general model considering oxide growth in aqueous solution under non-stationary conditions, and including parameters relative to the substrate alloys and transport *via* interstitial and vacancy positions.

A generalized oxide growth model has been developed. This model, which has a common basis with the PDM, takes into account the non-stationary conditions of oxide growth (potential drop evolution at the oxide solution interface and evolution of the electric field in the oxide film during oxide growth) and includes all the reactions involved in the oxide growth on metals and alloys (transport of anion *via* vacancies and cations *via* interstitial and vacancy positions). It is, to our knowledge, the first model able to describe the growth of oxide films on metals and alloys under non steady-state conditions. It also provides the link existing between the oxide film growth and release of alloy elements into the solution.

The application of this new model was exemplified here by the case of stainless alloy. In a subsequent paper, a numerical model for computed simulation of oxide growth is presented and validation tests on experimental kinetics of inner oxide growth obtained on Alloy 690 are reported.[15]

## Acknowledgments

The authors are grateful to EDF R&D, Center de Recherche des Renardières, Département MMC (D. Noël, F. Vaillant, T. Couvant), for partial financial support of this work.

## List of Symbols

| | |
|---|---|
| $\mathcal{F}$ | Faraday's constant (96484.6 C / mol) |
| $R$ | universal gas constant (8.31441 J / mol / K) |
| $k$ | Boltzmann's constant ($1.38.10^{-23}$ J / K) |
| $T$ | temperature (K) |
| $k_i$ | i reaction rate |
| $\phi_{m/f}$ | potential drop at the metal/oxide interface |
| $\phi_{f/s}$ | potential drop at the oxide/electrolyte interface |
| $\phi_f$ | potential drop inside the oxide film |
| $x$ | oxide film thickness |
| $F$ | electric field in the oxide layer |
| $V$ | potential drop in the metal/oxide/electrolyte system |
| $\Delta V$, $V_{app}$ | potential variation / applied potential |
| $C_i$ | concentration of charged species i (number of species / $m^3$) |
| $D_i$ | diffusion coefficient of charged species i ($m^2$ / s) |
| $J_i$ | flux of species i per unit area per unit time |
| $m$ | metallic atom |
| $M_M$ | metallic cation in the oxide |
| $V_M$ | cation vacancy in the oxide |
| $I_M$ | interstitial position in the oxide |
| $V_O$ | oxygen vacancy in the oxide |
| $v$ | vibration frequency of M atom |
| e | elementary charge |

## References

1. C. Wagner, *Z. Phys. Chem.*, **25**, B21 (1933).
2. N. Cabrera and N. F. Mott, *Rep. Prog. Phys.*, **12**, 163 (1948).
3. F. P. Fehlner and N. F. Mott, *Oxidation of Metals*, **2**, 59 (1970).
4. C. Y. Chao, L. F. Lin, and D. D. Macdonald, *J. Electrochem. Soc.*, **128**, 1187 (1981).
5. D. D. Macdonald, S. R. Baggio, and H. Song, *J. Electrochem. Soc.*, **139**, 170 (1992).
6. D. D. Macdonald, *Pure Appl. Chem.*, **71**, 951 (1999).
7. M. Bojinov, G. Fabricius, T. Laitinen, T. Saario, and G. Sundholm, *Electrochim. Acta*, **44**, 247 (1998).
8. M. Bojinov, G. Fabricius, T. Laitinen, K. Mäkelä, T. Saario, and G. Sundholm, *Electrochim. Acta*, **45**, 2029 (2000).
9. B. Diawara, Y. A. Beh, and P. Marcus, *J. Phys. Chem. C*, **114**, 19299 (2010).
10. K. N. Goswami and R. W. Staehle, *Electrochim. Acta*, **16**, 1895 (1971).
11. C. Lukac, J. B. Lumsden, S. Smialowska, and R. W. Staehle, *J. Electrochem. Soc.*, **122**, 1571 (1975).
12. C. Y. Chao and S. Smialowska, *Surf. Sci.*, **96**, 426 (1980).
13. M. Bojinov, A. Galtayries, P. Kinnunen, A. Machet, and P. Marcus, *Electrochim. Acta*, **52**, 7475 (2007).
14. D. D. Eley and P. R. Wilkinson, *Proc. Roy. Soc. (London) Ser. A*, **254**, 327 (1960).
15. K. Leistner, C. Toulemonde, A. Seyeux, and P. Marcus, submitted to *J. Electrochem. Soc.*
16. A. Seyeux, V. Maurice, and P. Marcus, *Electrochemical and Solid State Letters*, **12**, C25 (2009).
17. J. Panther, Thèse de doctorat de l'Institut National Polytechnique de Toulouse (2002).
18. J. Panther, M. Foucault, J. M. Clou, P. Combrade, and B. Viguier, Proceedings of corrosion 2002, Denver (2002).
19. J. Panther, M. Foucault, P. Combrade, K. Wolski, and T. Magnin, *Proceedings of the Ninth International Symposium On Environmental Degradation of Metals in Nuclear Power Systems – Water Reactors*, Newport Beach (1999).
20. A. Machet, Thèse de l'Université Pierre et Marie Curie, Paris VI (2004).
21. A. Machet, A. Galtayries, S. Zanna, L. H. Klein, V. Maurice, P. Jolivet, M. Foucault, P. Combrade, P. Scott, and P. Marcus, *Electrochim. Acta*, **49**, 3957 (2004).
22. A. Machet, A. Galtayries, P. Marcus, P. Combrade, P. Jolivet, and P. Scott, *Surface and Interface Analysis*, **34**, 197 (2002).
23. L. Marchetti, Thèse de doctorat de l'Ecole Nationale Supérieure des Mines de Saint-Etienne (2007).